ACS APPLIED ELECTRONIC MATERIALS

pubs.acs.org/acsaelm Article

Highly Stable, Pretilted Homeotropic Alignment of Liquid Crystals Enabled by In Situ Self-Assembled, Dual-Wavelength Photoalignment

Vineet Kumar, Zhiqiu Ye, Haodong Jiang, Yue Shi, Ke Li, Davy Gérard, Dan Luo, Quanquan Mu, and Yan Jun Liu*

Cite This: *ACS Appl. Electron. Mater.* 2020, 2, 2017−2025 Read Online

ACCESS | Metrics & More | Article Recommendations | Supporting Information

ABSTRACT: Homeotropic alignment of liquid crystals (LCs) is one of the key modes used in commercial liquid crystal displays (LCDs) due to its advantages, such as high contrast ratios and fast response speed. Here, we report stable homeotropic LC alignment with a small pretilt angle in a nematic, negative LC host doped with additives including self-aligning agents, photoresponsive azo dyes, and reactive mesogen via an in situ self-assembled, dual-wavelength photoalignment approach. The underlying mechanism of stable, pretilted homeotropic LC alignment was further analyzed in detail. The achieved pretilted homeotropic LC cells are very stable against heat and UV light exposure and demonstrate excellent electro-optical characteristics. The experimental results show that such a noncontact, simple homeotropic alignment technique has big potential in many applications, such as high-quality LCDs, spatial light modulators, and other optoelectronic devices.

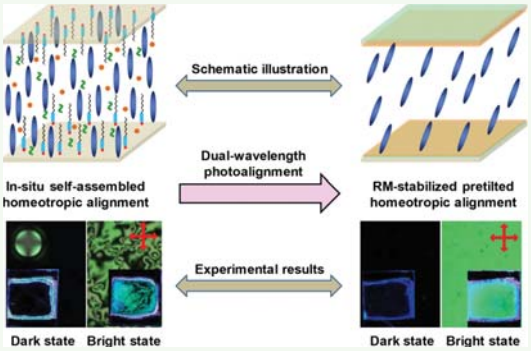

KEYWORDS: *liquid crystals, vertical alignment, self-assembly, azo dyes, photoalignment, polymer stabilization*

INTRODUCTION

Liquid crystal displays (LCDs) are ubiquitous in the present technological society ranging from day-to-day smart phones to different home appliances such as TVs, computers, etc. The wide use of LCDs is possible only because of the key advancement in LC alignment control technologies. Homeotropic and homogeneous alignments of LCs have been commercially successful in device fabrications because of great advantages including high contrast ratios, fast response speeds, and simple and easy fabrication processes. So far, mechanical rubbing of polyimide-coated conductive indium-tin-oxide (ITO) substrates is the major LC alignment technique. Rubbing of polyimide consists of multi-step processes such as coating and soft and hard baking along with the drawbacks like dust creation, surface damage, or electrostatic charge generation, greatly limiting its application for high-quality displays. Several alternative noncontact alignment techniques have been proposed, such as those of photoalignment,[1−3] self-assembled monolayers (SAMs),[4,5] oxide evaporation,[6] nanopatterns,[7−9] etc. to get rid of the shortcomings involved in the rubbing technique. The noncontact LC alignment systems consisting of nanoparticles or surface-active agent dispersion in the LC host have been reported to achieve macroscopic homeotropic or homogeneous alignments.[10−14] Surface-active agents (amphiphilic molecules) like hexadecyl trimethyl ammonium bromide (HTAB) in negative LC hosts interact with ITO substrates and result in homeotropic alignment due to molecular self-assembly at the interfaces.[15] The amphiphilic molecules usually contain a polar anchoring group and a flexible long alkyl chain in which the polar anchoring group interacts with the ITO surface, leaving the flexible long alkyl chain in the LC bulk to homeotropically align the LC molecules.[16−18] In addition, nanoparticles have been also reported as automatic LC alignment-inducing agents where plasmonic or nonplasmonic molecules like Au, Ni, ZnO, CuS, CdSe, POSS, or fullerene (C_{60}) and carbohydrate-based dopants[19−21] were mixed with LCs in small amounts. Upon cooling from an isotropic to a nematic phase of such LC−nanoparticle mixtures, phase separation occurs. A layer of self-aligning agents (SAAs) is formed, which further determines a specific orientation of LCs. In most cases, nanoparticles break the continuity of the rotational symmetry by producing defects, hence resulting in

Received: April 10, 2020
Accepted: June 16, 2020
Published: June 16, 2020

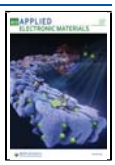

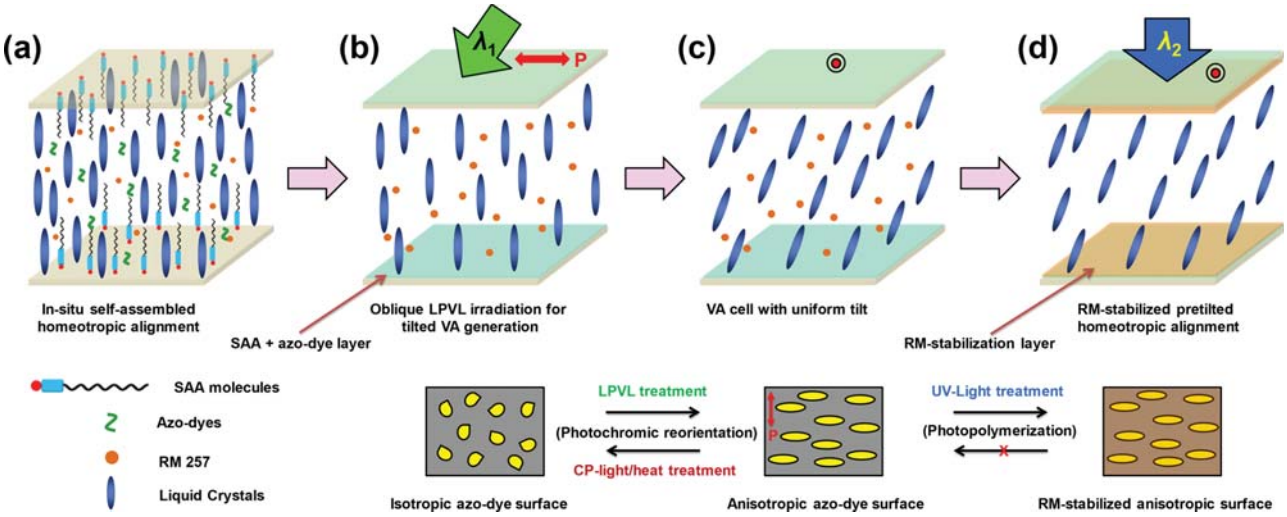

Figure 1. Schematic illustration of our proposed in situ self-assembled, dual-wavelength photoalignment. (a) In situ self-assembled pristine homeotropic cell prior to any light treatment that contains randomly distributed additives in the LC and ITO/LC interfaces after adsorption. Additives like SAA molecules, azo dyes, and RMs are represented by a blue rectangular block containing a red circular polar unit and a black flexible alkyl chain, zigzag green molecules, and brown circular dots, respectively. Elongated eclipses in purple color represent the LC molecules. (b) Oblique LPVL treatment of the azo dye with a λ_1 wavelength to create a pretilt angle in homeotropic cell. The box below illustrates the corresponding isotropic azo-dye surface. (c) Uniformly pretilted homeotropic LC alignment with an anisotropic azo-dye composite layer at the surface oriented perpendicular to the polarization direction of visible light. Corresponding azo-dye anisotropic surface due to LPVL treatment and photoreorientation boxed below, which possesses a reversible nature and can be randomized to the initial stage upon thermal relaxation or light exposure. (d) Alignment stabilization by RM polymerization using UV light with a λ_2 wavelength in the nematic phase of LCs. The RM layer forms a thin polymer coating (orange color) that controls the alignment. The anisotropic azo-dye surface becomes irreversible in nature since a polymer layer is formed on top of the composite layer due to UV-light-induced RM polymerization and further seizes the reorientation property of the azo dye molecules, as shown in the box below. Double-ended arrow in (b) and the arrow heads in (c) and (d) indicate the polarizer and LC director directions, respectively.

homeotropic alignment of LCs. The resulting LC cells possess remarkable electro-optical properties, such as memory effects, frequency modulation responses, fast responses, and low driving voltages.[22−25] However, there also exist some unresolved issues, such as poor interactions with LCs, aggregation-induced light leakage, and unstable LC alignment against heat, light, and moisture, hence culminating in poor device quality. In order to resolve these drawbacks, we propose a new noncontact alignment technique that combines photoalignment with self-aligning agents (SAAs).

As it is known, photoalignment is an important and attractive noncontact LC alignment method due to photopatternable characteristics[26−30] and a clean and simple process. Recently, polyimide-free homeotropic or homogeneous photoalignment systems have been realized using photopolymerizable monomers or mixed monomers upon suitable light irradiation.[31−33] Photopolymerization of monomers upon linearly polarized light irradiation results in uniform homogeneous alignment of LCs. The resulting alignment is quite stable with improved electro-optical properties. In addition, it only requires low processing temperatures below 200 °C, making it compatible for flexible LCDs. To realize the use of the photoalignment process in combination with SAA systems, photochromic materials (for instance, azo dyes) will be quite suitable due to reversible cooperative conformational changes of azobenzene upon light irradiation of different wavelengths.[34−39] Azo-dye molecules in combination with amphiphilic or hydrophilic molecules can self-assemble on the ITO interfaces, which can further tune the anchoring properties or boundary conditions of the interfaces for a specific orientation of LCs with light irradiation.[40,41] Furthermore, the doping of reactive mesogen (RM) molecules in the system along with azo dyes has been reported to enhance alignment stabilization upon UV irradiation, resulting in an irreversible orientation of LCs.[42−44]

In this work, we report highly stable, pretilted homeotropic LC alignment in a nematic, negative LC host doped with SAA molecules, azo dyes, and RM additives via an in situ self-assembled, dual-wavelength photoalignment approach. Our approach combines two different noncontact LC alignment methods (self-assembly and photoalignment) with two major processes. In the first process, the amphiphilic molecules interact with the ITO surface, spontaneously resulting in homeotropic LC alignment. In the second process, the photoresponsive azo dyes sensitive to visible light and UV-polymerizable RM molecules are utilized to perform dual-wavelength photoalignment with the purpose to create a small pretilt angle and stabilize alignment, respectively. A uniform pretilt angle of 0.7° has been achieved at the end of the dual-wavelength irradiation process, and the obtained alignment is quite stable against heat and light treatment. Such a noncontact, simple homeotropic alignment technique is very promising for applications including high-quality LCDs, spatial light modulators, and other optoelectronic devices.

■ DESIGN PRINCIPLE

Figure 1 schematically describes the design principle of our proposed in situ self-assembled, dual-wavelength photoalignment that combines self-assembly and dual-wavelength photoalignment. First, in situ homeotropic LC alignment occurs due to a random distribution of SAA and azo-dye molecules adsorbed at the ITO surface upon the infiltration of all the

https://dx.doi.org/10.1021/acsaelm.0c00295
ACS Appl. Electron. Mater. 2020, 2, 2017−2025

well-mixed materials, as shown in Figure 1a. In our design, we purposely choose a photochromic azo dye that is sensitive to visible light. Upon linearly polarized visible light (LPVL) irradiation, the azo dye can reorient the LC molecules due to its dichroic absorption and subsequent *trans*−*cis* isomerization. Continuous irradiation of LPVL increases the population of azo-dye molecules falling under the perpendicular direction of light polarization, which makes it less likely to go under transition for isomerization and results in the average orientation of azo-dye molecules perpendicular to the polarization direction of light. As a result, upon LPVL irradiation, the isotropic layer of adsorbed azo dyes on the ITO surface becomes anisotropic in nature and induces LC alignment perpendicular to the light polarization direction. Figure 1b shows the oblique LPVL (λ_1) treatment to induce LCs' photoalignment. For simplicity, a composite layer (labeled in light green color) of SAA and azo dye molecules is formed due to interfacial adsorption on the ITO surface, which further results in self-assembly-induced homeotropic LC alignment, as shown in Figure 1b. Separately, random distributions of azo-dye molecules at the surfaces are represented by yellow distorted circular dots in a box shown below in Figure 1b. LPVL treatment is carried out using a tilted light source at 65° with respect to the substrate normal. Upon LPVL treatment, a small pretilt angle will be created from the normal orientation of the LC director, as shown in Figure 1c. The observed LC director alignment is perpendicular to the polarization direction of light as confirmed by using quarter wave plates. The corresponding azo-dye surface becomes anisotropic in nature as represented by the azo dye in yellow-colored elongated eclipses aligned along one direction due to LPVL treatment (see the box below Figure 1c), which is responsible for the pretilt angle generation. RM molecules uniformly distributed in the LC bulk remain unperturbed at the end of the LPVL photoalignment process due to the screening of UV light by using a bandpass filter. At this stage, the alignment is reversible in nature, meaning a nonstable alignment state. The stabilization of the alignment can be achieved by RM polymerization via UV-light irradiation. The LPVL and UV-light treatment processes are therefore referred as dual-wavelength photoalignment. The RM polymerization is initiated by a photoinitiator used in trace amounts upon unpolarized UV-light (λ_2) irradiation at room temperature.[43−46] Stabilization of LC alignment by RM polymerization results in the formation of a thin polymer layer on top of the composite layer of SAA and azo-dye molecules, as shown in Figure 1d. The RM stabilization layer seizes the freedom of azo dyes' reorientation capability influenced by the reversible photoisomerization process.[46,47] Here onward, the new RM layer commands the LC alignment and endures irreversible LC orientation along a specific direction. The formed RM layer over the composite layer of additives is represented in light brown color, as shown below Figure 1d. Therefore, our proposed in situ self-assembled photoalignment approach paves a new way to control the processes of LC alignment and stabilization separately and prevents the inevitable intermeddling when only a single wavelength of light is used.

EXPERIMENTAL SECTION

Materials. A nematic LC, HNG715600-100 (Jiangsu Hecheng Advanced Materials Co.) with negative dielectric anisotropy was used as the host LC in our experiments. Amphiphilic molecules, 4′-octylbiphenyl-4-carboxylic acid (OBA) (MedChemExpress) and lauryl gallate (LG) (Sigma Aldrich), were used as the SAAs for in situ self-assembled LC photoalignment. Visible-light-sensitive azo-dye methyl red (MR) (Sigma-Aldrich) and UV-polymerizable reactive mesogen RM257 (Jiangsu Hecheng Advanced Materials Co.) were used as photoalignment and stabilizing agents of LC alignment. Trace amounts of photoinitiator Irgacure 651 (Jiangsu Hecheng Advanced Materials Co.) were doped in the system in order to initiate the photopolymerization of RM257. All the chemicals involved in this system were used as received without any further modifications or purifications. The one-bottle approach of this experimental system consists of 0.1 wt % LG or OBA, 0.2 wt % MR, and 0.1 wt % RM257 with trace amounts of Irgacure 651 in the LC host, which were homogeneously mixed by stirring at the isotropic temperature for 15 min. The details of the LC host and entities involved in the experiment are shown in Figure 2 with their chemical structures.

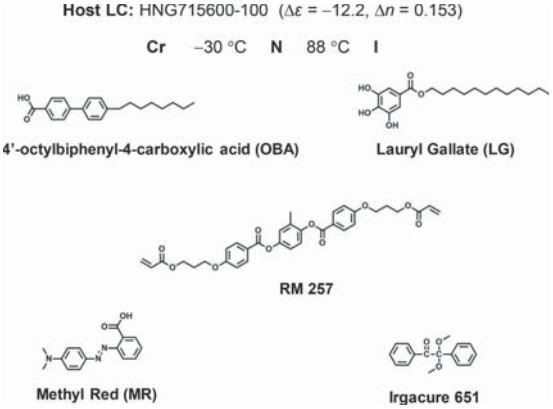

Figure 2. Details of liquid crystal and chemical additives used in the system as a one-bottle experimental approach.

The UV−vis absorption spectrum of MR is presented in Figure S1 in the Supporting Information. MR constituents extended π conjugation along with electron-donating and withdrawing functional groups, which shift the absorption band in the visible light spectrum range.[48−50] The MR absorption ranges from 390 to 550 nm, showing significant visible light absorption that is purposely suitable for our designed dual-wavelength in situ photoalignment approach. The photochromic properties of the azo dye under the influence of LPVL irradiation were also examined using the absorption spectra of an azo-dye coated film on the ITO substrate before and after photoalignment (see Figure S2). It is clearly visible that the absorption spectrum exhibits a considerable decrease near 470 nm and increase near 380 nm, reflecting the occurrence of a *trans*−*cis* isomerization process. The isomerization process upon LPVL irradiation significantly decreases the population density of the *cis*-form molecules and simultaneously increases the population density of the *trans*-form molecules. The change of the absorption spectra indicates the formation of an anisotropic azo-dye layer, which could further induce LC alignment.

LC Cell Fabrications. Commercially available ITO-coated conductive glass substrates were used in our experiments. They were cleaned by sonication in a detergent solution, deionized water, acetone, and 2-isopropanol (IPA) in sequence at least twice and then dried in the oven at 80 °C overnight. Two pieces of the dried ITO glass, without any coatings, were assembled to an LC cell with the optical adhesive NOA65. The cell gap was controlled to be 10 μm using the ball spacer. The homogeneous host−guest mixture was injected in the cells by capillary action at the isotropic temperature of 110 °C and then slowly cooled down to the room temperature. Homeotropic alignment of LCs was spontaneously achieved upon completion of the cooling-down process. Various material recipes of

https://dx.doi.org/10.1021/acsaelm.0c00295
ACS Appl. Electron. Mater. 2020, 2, 2017−2025

different ratios and concentrations have been tested in order to achieve the optimal alignment condition.

In Situ Alignment Control Using Photoalignment. The in situ self-assembled homeotropic LC cells were further subjected to LPVL treatment at isotropic temperature. Visible light illumination of the cell was carried out using a high-pressure 200 W Hg lamp (OmniCure Series 2000) as a light source and an Instec mK2000 temperature controller with a hot stage to maintain an elevated temperature of 110 °C. Collimated LPVL irradiation was carried out with an oblique incident angle of 65° with respect to the cell normal. An optical bandpass filter (400−700 nm, Thorlabs) was used to ensure only visible light irradiation of the cell for photoalignment. A mask with a circular hole was used to demonstrate uniform monodomain pretilt alignment for the VA cell at the end of the photoalignment step as shown in the later section. The obtained pretilt angle of the homeotropic cell was measured using a modified LC rotation method with an optical setup assembled in the laboratory and using the instrument PAMS 200 (Sesim Photonics Technology, S. Korea).

Stabilization of Tilted Homeotropic Alignment. As the idea of dual-wavelength photoalignment suggests, after the completion of in situ photoalignment by visible light, the second-step irradiation with UV light at room temperature was performed to stabilize the LC alignment. Upon UV light irradiation, photopolymerization of RM molecules took place and a stabilization layer was formed on top of the composite layer of azo-dye and SAA molecules. The UV light illumination was done by a UV-LED point light source (LOTS, UVEC-4II) in order to initiate the RM polymerization and polymer stabilization layer formation to attain irreversible alignment of LCs. The stabilization of tilted homeotropic alignment was achieved upon completion of RM polymerization using UV light exposure, which significantly cures the RM molecules. The UV light source with the wavelength range of 350−380 nm was used for RM polymerization.

Characterization of the Polymer Stabilization Layer. The achieved homeotropic cells were kept in a co-solvent system of hexane and chloroform for 24 h to remove the LCs, unreacted monomers, and other additives. Cells were dismantled using sharp edge blades, and top and bottom ITO substrates were separated for FESEM and other characterizations. The surface morphologies were observed under a field emission scanning electron microscope (FESEM; GeminiSEM 300-71-10, Zeiss) in order to analyze the RM stabilization layers. The contact angle was measured with a contact angle detector (Powereach JC2000-99B, Shanghai Zhongchen Digital Technology Apparatus Co.) that helps in obtaining information regarding the wettability nature of the RM polymer layer.

Optical Characterizations. The absorption spectrum for methyl red azo-dye of ~10^{-5} M solution in ethanol was acquired using a UV−vis spectrophotometer (Jasco, ARSN-733). A polarized optical microscope (POM) was used for LC alignment and its texture monitoring. A POM instrument (Nikon Eclipse, Ci POL) was equipped with a Nikon DS-Fi2 CCD camera for optical image acquisition. The electro-optical properties were measured using a 633 nm He−Ne laser (Research Electro-Optics Inc.), a photodetector (PM100A, Thorlabs), and a function generator (DG4102, Rigol). The voltage-response time optical properties were measured using an LC electro-optical complex tester equipped with a white light source (ZKY-LCDE0-2, Chengdu Shijizhongke Equipment Co.). The LC cell was switched under a crossed polarizer and applied voltage of the square wave mode with a frequency of 1 kHz using a power amplifier (PZD350A, Trek). The response time was measured using an oscilloscope (DPO2024, Tektronix).

RESULTS AND DISCUSSION

From our designed idea, once the LC cell was loaded with the mixture at a temperature above the clearing point (T_{NI}) and then slowly cooled down to the room temperature, homeotropic alignment was spontaneously formed inside the LC cell. The hydrophilic ends of the SAA molecules, acting as an anchoring unit, interact with the ITO surface, while the SAA molecules' flexible alkyl chains possess affinity to the LC bulk and orientate perpendicular to the surface, further influencing the overall LC alignment. The POM and macroscopic images in Figure 3a illustrate the pristine

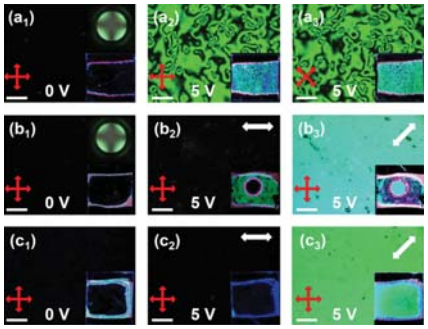

Figure 3. Polarized optical images of a (a_1−a_3) pristine, (b_1−b_3) LPVL-treated, (c_1−c_3) UV-treated homeotropic cell at a 0° sample stage rotation with no driving voltage (a_1, b_1, and c_1), at a 0° sample stage rotation with the driving voltage of 5 V (a_2, b_2, and c_2), and at a 45° sample stage rotation with the driving voltage of 5 V (a_3, b_3, and c_3). The top right insets in (a_1) and (b_1) show the conoscopic image. All the bottom right insets illustrate the complete sample photos observed under two crossed polarizers. The scale bar at the bottom left corner in each image is 100 μm.

homeotropic alignment of LCs before dual-wavelength treatment. Figure 3a_1 shows the observed POM images under two crossed polarizers at a 0° sample stage rotation with no applied voltage, illustrating a complete dark state. The top right inset in Figure 3a_1 shows the conoscopic image, confirming the homeotropic LC alignment. Figure 3a_2,a_3 shows the POM images at 0° and 45° sample stage rotations with an applied voltage of 5 V. A nonuniform bright field can be clearly observed from both POM images, indicating a random distribution of LC directors upon electrical switching. At the initial homeotropic state, all the LC molecules are aligned perpendicular to the substrate without a pretilt angle. Upon applying a driving voltage, the LC molecules will re-orientate randomly without any preferred and uniform direction, hence resulting in an observed nonuniform bright field. Figure 3b shows the case after LPVL treatment. Figure 3b_1 demonstrates similar observed phenomena as Figure 3a_1, confirming that the homeotropic alignment was still kept after LPVL treatment. However, in contrast to Figure 3a_2,a_3, Figure 3b_2,b_3 demonstrates completely dark and uniform bright POM images for the LPVL-irradiated circular area under the same driving voltage of 5 V, indicating the creation of a pretilt angle. Only with a pretilt angle does uniform, unidirectional re-orientation of all LC molecules occur upon switching. The generated pretilt angle was measured to be 0.5° upon LPVL treatment with the exposure dose of 10.8 J/cm^2 (6 mW/cm^2 for 30 min). A black masking tape with a circular opening hole was used to obtain the LPVL photoalignment effect, illustrating clearly distinguishable aligned and nonaligned areas, as shown in the bottom right insets in Figure 3b_2,b_3. The achieved monodomain LC alignment in the circular region confirms a uniform pretilt orientation of LCs in the self-assembled homeotropic cell. The obtained LPVL photoalignment effect is reversible in nature and can be easily erased even at room temperature in several hours or overnight due to the thermal relaxation of the azo-dye molecules. A well aligned cell

https://dx.doi.org/10.1021/acsaelm.0c00295
ACS Appl. Electron. Mater. 2020, 2, 2017−2025

after LPVL photoalignment got randomized after keeping it overnight in an ambient environment, as shown in Figure S2 in the Supporting Information. For practical applications, stabilization of LC alignment is the essential prerequisite criteria. Therefore, RM polymerization was further carried out under UV-light irradiation in order to stabilize the LC alignment. Figure 3c shows the case after the UV-light treatment. Again, Figure 3c_1 demonstrates similar observed phenomena to those of Figure 3a_1,b_1, confirming that there is no alignment change after both LPVL and UV-light treatment. Correspondingly, Figure 3c_2,c_3 shows similar behavior to that in Figure 3b_2,b_3. The RM monomers were polymerized using unpolarized UV light with an exposure dose of 40.5 J/cm^2 (15 mW/cm^2 for 45 min) at room temperature, essentially higher than that used for the alignment process to ensure complete polymerization quickly and minimize any alignment deformation. During the stabilization process, a thin polymer layer was formed over the composite layer of the SAA and azo-dye additives, which further modified the interfaces and rendered irreversible, permanent alignment of LCs. A large-area, uniform monodomain pretilted homeotropic alignment can be finally achieved, as shown in the bottom right insets in Figure 3c. Stability of LC alignment against extreme heat and light exposure was further tested. Heat exposure at 110 °C for several hours slowly degrades the LC alignment starting from the boundaries near the spacers as shown in Figure S3. Gradually, LC alignment over the large area was lost; it might be caused by the freed azo-dye molecules, which diffuse through the thin polymerized RM layer from the ITO/LC interface, gradually go into the bulk LC, and damage the uniform alignment during the heating process. However, this testing temperature is far above the clearing point of the widely used LCs. In contrast, unpolarized UV-light treatment with a uniform intensity at 30 mW/cm^2 for 2 h at room temperature did not significantly affect the LC alignment, and stability was intact over the large area as shown in Figure S4. As a result, the efficient stable homeotropic LC alignment was successfully demonstrated using our proposed in situ self-assembled photoalignment approach. The room temperature stability of obtained LC alignment was permanent with the increased pretilt angle of 0.7° from 0.5° after RM stabilization. The polymer stabilization layer is also known to reduce transient disclinations or defect formation and hence exhibits enhanced switching behavior for LC devices. A pretilt angle will define a well-determined direction for the LC reorientation once the electric field is applied, and hence, it can improve the threshold voltage and response time for the device.[51] However, a large pretilt angle can lead to a light leakage at the dark state. The light leakage will then lower the contrast ratio of the device. Therefore, homeotropic LC alignment with a small pretilt angle is highly desired, which can not only improve electro-optic characteristics but also keep a high contrast ratio of a device. It is worth mentioning that the pretilt angle could be further optimized by varying the LPVL irradiation dose and RM concentrations.

To further confirm the formation of the stabilization layer and understand the minute morphological details, we carried out the FESEM observation of the ITO substrate surface. The observed surface morphologies for the top and bottom ITO substrates were almost the same. Figure 4 shows the surface morphologies of the top substrate observed under FESEM for the samples with the RM257 concentrations of 0.05 and 0.1 wt %. From Figure 4, a thin RM stabilization layer can be clearly

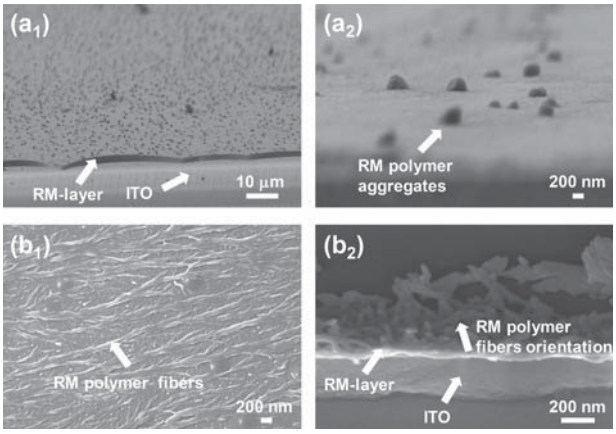

Figure 4. (a_1) Low- and (a_2) high-magnification cross-sectional SEM images illustrating the surface morphologies of the sample with the RM257 concentration of 0.05 wt %, which were observed with the sample stage tilted at 10°. (b_1) Top and (b_2) cross-sectional SEM images for the sample with the RM257 concentration of 0.1 wt %.

observed over the ITO substrates. For the case of a low RM257 concentration in Figure 4a_1,a_2, there are some isolated protrusions like RM aggregates decorated over the stabilization layer. The RM aggregates have an averaged particle size of 200−400 nm. The random distribution of RM aggregates corresponds to the morphological evidence of a factor responsible for homeotropic alignment as it breaks the boundary symmetry conditions of LCs. Morphological observations imply that the nature of alignment formation could be similar to that of SAMs or nanoparticle doping systems that exert homeotropic alignment of LCs.[52,53] The low RM257 concentration case could not provide much information regarding the anisotropic nature of the RM stabilization layer or LC director orientation. In order to further examine the morphological details and LC director orientation, a sample with a high RM257 concentration of 0.1 wt % was used for the alignment stabilization. Figure 4b_1,b_2 shows the top and cross-sectional views of the top ITO substrate for the sample with the high RM257 concentration. The top view image of the RM polymer layer in Figure 4b_1 shows the orientation of polymer fibers or bundles running along one direction, which is perpendicular to the polarization direction of LPVL and concurrent to the LC director orientation. The cross-sectional image in Figure 4b_2 clearly displays the presence of vertically oriented RM polymer fibers closely packed together. The vertically tilted orientation of columnar RM polymer fibers was formed due to a tilted homeotropic orientation of LC directors, which guided the polymer templating during polymerization along the vertical direction. The tilted vertically oriented polymer fibers support the experimental observations of alignment stabilization for the in situ self-assembled homeotropic cell using the dual-wavelength approach. Polymer layers formed at the ITO/LC interfaces significantly improve the anchoring strength and lead to stabilization of LC alignment. As reported,[41,54] during the RM polymerization process, polymerization-induced phase separation occurs, and the polymerized RM aggregates will migrate toward the interface and be immobilized over the SAA layer, forming the stabilization layer for the irreversible homeotropic alignment. The formed RM stabilization layer increases the hardness and roughness of the alignment surface,

https://dx.doi.org/10.1021/acsaelm.0c00295
ACS Appl. Electron. Mater. 2020, 2, 2017−2025

hence increasing the surface anchoring energy of the alignment layer. The passive nature of polymer layers makes them resistant to the damaging factors that can perturb the LC alignment conditions. It has been reported that such systems with RM-stabilized LC alignment can maintain the anchoring strength under the applied AC-field stress test for 24 h as it is a crucial factor to determine industrial applications of LC devices.[47] If the anchoring strength is not strong enough, the relaxation process will become very slow. As reported,[47] the AC-field stress test for an IPS cell without RM stabilization showed defect creation and weak anchoring strength of LCs at the surface; in contrast, the same test with RM stabilization accomplished fast and complete relaxation of LCs, confirming the sufficiently strong anchoring induced by the RM layer. The RM stabilization layer therefore acts as a new alignment layer with both strong anchoring strength and an irreversible nature as required for most of the LCD devices.

It is evident that interfacial modification of the ITO surfaces plays a key role for the homeotropic LC alignment. The wetting properties of the RM stabilization layer were therefore investigated using contact angle measurement to confirm the interfacial modification of surface anchoring capability. Figure 5a–c shows the measured contact angles of 55°, 80°, and 85°

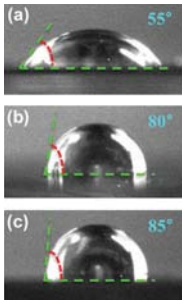

Figure 5. Measured contact angles for (a) the bare ITO surface and RM-stabilization surfaces with (b) low and (c) high RM257 concentrations, respectively. Water with a volume of 1 mL was used as the solvent for the contact angle measurement.

for the bare ITO surface and RM-stabilization surfaces with low and high RM257 concentrations, respectively. The contact angle increases with the polymerization of RM at the ITO/air interface because it decreases the hydrophilicity of the ITO surface due to the polymer coating. The increasing RM concentration further reduces the hydrophilicity, and it tends to be hydrophobic in nature. The modified nature of the coated surface renders ideal support for the homeotropic alignment. In other words, the anchoring energy of the bare ITO surface was significantly changed from enabling a homogeneous orientation of LCs to homeotropic. It is expected that the anchoring energy after the RM stabilization will be higher than that of the pristine cell without polymer stabilization.[55] The increase in the anchoring energy of the RM stabilization layer compared to the bare ITO layer can be attributed to the increased surface roughness.[56] From Figure 5, the significant change in the contact angle confirms the hydrophilic to hydrophobic transition of the surface nature, which supports the evidence of pretilted homeotropic alignment stabilization by the RM layer.

The electro-optical properties of the pretilted homeotropic LC cell were finally tested. The uniformity of LC alignment was characterized by switching the cell with a driving voltage of 5 V and placing it under two crossed polarizers. By keeping the LC cell at fixed position while rotating either the polarizer or analyzer, sinusoidal variation of darkness and brightness at the interval of 45° can be observed, as shown in Figure 6a, confirming the uniaxial tilted orientation of the LC director. Figure 6b shows the voltage-dependent transmittance ($V-T$) curve of the cell, which shows the similar characteristics as conventional PI-based systems. The threshold voltage was ~2.4 V, which was lower than that of the PI-based systems as reported previously.[57,58] The transmittance increases as the applied voltage was increased from 0 to 3.5 V and then gradually decreased to an almost saturated state at 5 V. The gradual decrease in the transmittance after 3.5 V may be due to the large cell gap, which needs to be optimized in accordance with the $d\Delta n$ parameter. Moreover, the voltage-dependent response time of the pretilted homeotropic cell was measured under a 1 kHz AC voltage with a 3.5 V_{pp} amplitude. The measured rising and falling time from Figure 6c,d was ~68 and ~38 ms, respectively. The response time for this device is expected to be faster than that of the PI-based devices since the LC molecules are in direct contact with the ITO surface and also contain a predetermined director tilt with a biased nature of alignment. A high contrast ratio of 593:1 for the device was achieved. These obtained results are in good agreement with the expectations and could be further optimized for specifically designed systems based on in situ self-assembled homeotropic alignment.

The surface anchoring energy is an important parameter for an LC cell as it affects not only the LC alignment but also the electro-optic properties (for instance, threshold voltage and response time). Various experimental techniques have been developed for measuring the anchoring energy. Here, we used the recently suggested reliable RV (retardation vs voltage) techniques.[59,60] Figure 7 plots the measured $(R/R_0 - 1)(V - V')$ as a function of voltage. The experiment was carried out with a He–Ne laser (λ = 633 nm) at room temperature. By fitting the slope of the linear curve, the anchoring strength is deduced between V_{min} and V_{max}. Here, V_{min} = 9 V (~4 V_{th}) and V_{max} = 20 V have been used to calculate the anchoring energy of the 10 μm cells with good linear fitting. The obtained anchoring strengths for a homeotropic cell before light treatment and after RM stabilization were 4.410×10^{-5} and 1.418×10^{-4} J/m^2, respectively. The change of nearly 1 order of magnitude in the anchoring energy shows that surface anchoring energy of RM stabilized cell is much stronger than the pristine one, indicating big potential for many applications, such as high-quality LCDs, spatial light modulators, and other optoelectronic devices.

CONCLUSIONS

In summary, we have successfully demonstrated highly stable homeotropic LC alignment with a small pretilt angle in a nematic, negative LC host doped with additives including self-aligning agents, photoresponsive azo dyes, and reactive mesogen via an in situ self-assembled, dual-wavelength photoalignment approach. The underlying mechanism of stable, pretilted homeotropic LC alignment has been discussed in detail. Amphiphilic SAA molecules resulted in self-assembled homeotropic LC alignment that pave the way for polyimide-free LC alignment. More importantly, the addition of photoresponsive azo-dye and RM molecules in the materials system played a critical role in subsequent interfacial modification using the dual-wavelength approach to achieve

https://dx.doi.org/10.1021/acsaelm.0c00295
ACS Appl. Electron. Mater. 2020, 2, 2017–2025

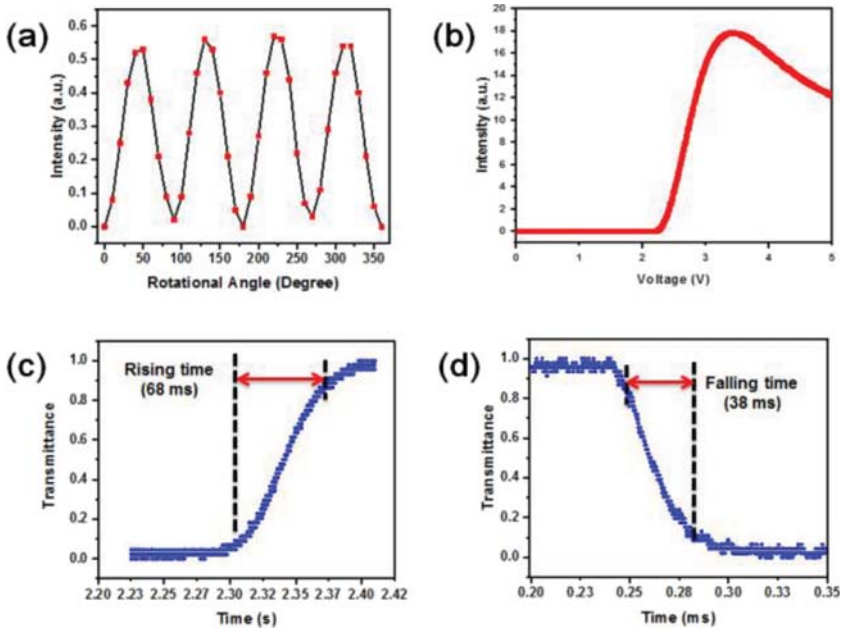

Figure 6. Electro-optical and switching characteristics of the LC cell after RM stabilization. (a) Sinusoidal variation of darkness and brightness at the interval of 45° by rotating either the polarizer or analyzer. (b) Voltage-dependent transmittance curve. (c, d) Rising and falling time measurement under the driving voltage of 3.5 V_{PP}.

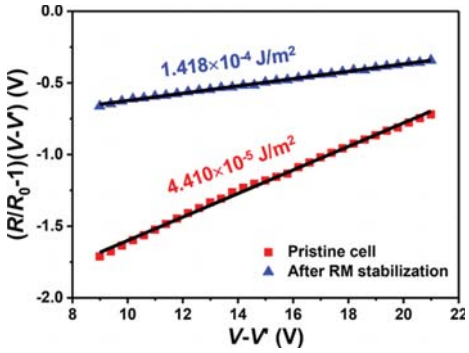

Figure 7. Measured anchoring energy for the homeotropic cell before (pristine) and after RM stabilization with the pretilt angle from the voltage-dependent RV curves.

in situ pretilted photoalignment and stabilization, respectively. The achieved pretilted homeotropic LC cells are very stable against heat and UV light exposure and demonstrate excellent electro-optical characteristics. Our proposed in situ self-assembled, dual-wavelength photoalignment technique is simple and efficient, which could be the game changer in terms of production cost, processing time, and complexity compared to mechanical rubbing. Such a noncontact, simple homeotropic alignment technique has big potential in many applications, such as high-quality LCDs, spatial light modulators, and other optoelectronic devices.

■ ASSOCIATED CONTENT

Supporting Information

The Supporting Information is available free of charge at https://pubs.acs.org/doi/10.1021/acsaelm.0c00295.

UV−vis absorption spectrum of the azo dye solution and polarized photographs of the LC cells for stability test (PDF)

■ AUTHOR INFORMATION

Corresponding Author

Yan Jun Liu − *Department of Electrical and Electronic Engineering, Southern University of Science and Technology, Shenzhen 518055, China; State Key Laboratory of Applied Optics, Changchun Institute of Optics, Fine Mechanics and Physics, Chinese Academy of Sciences, Changchun 130033, China;* orcid.org/0000-0001-8724-0434; Email: yjliu@sustech.edu.cn

Authors

Vineet Kumar − *Department of Electrical and Electronic Engineering, Southern University of Science and Technology, Shenzhen 518055, China*

Zhiqiu Ye − *Department of Electrical and Electronic Engineering, Southern University of Science and Technology, Shenzhen 518055, China*

Haodong Jiang − *Department of Electrical and Electronic Engineering, Southern University of Science and Technology, Shenzhen 518055, China; Harbin Institute of Technology, Harbin 150001, China*

Yue Shi − *Department of Electrical and Electronic Engineering, Southern University of Science and Technology, Shenzhen 518055, China; School of Physical Science and Technology, Ningbo University, Ningbo 315211, China*

Ke Li − *Department of Electrical and Electronic Engineering, Southern University of Science and Technology, Shenzhen 518055, China; Light, Nanomaterials, & Nanotechnologies (L2n), Université de Technologie de Troyes & CNRS ERL 7004, 10004 Troyes, France*

Davy Gérard − *Light, Nanomaterials, & Nanotechnologies (L2n), Université de Technologie de Troyes & CNRS ERL 7004, 10004 Troyes, France;* orcid.org/0000-0003-4789-9888

https://dx.doi.org/10.1021/acsaelm.0c00295
ACS Appl. Electron. Mater. 2020, 2, 2017−2025

Dan Luo − *Department of Electrical and Electronic Engineering, Southern University of Science and Technology, Shenzhen 518055, China;* orcid.org/0000-0003-2117-0570

Quanquan Mu − *State Key Laboratory of Applied Optics, Changchun Institute of Optics, Fine Mechanics and Physics, Chinese Academy of Sciences, Changchun 130033, China*

Complete contact information is available at: https://pubs.acs.org/10.1021/acsaelm.0c00295

Notes

The authors declare no competing financial interest.

■ ACKNOWLEDGMENTS

This work was supported in part by the Natural Science Foundation of Guangdong Province (grant nos. 2017A030313034 and 2018A030310224), Shenzhen Science and Technology Innovation Commission (grant no. JCYJ20170817111349280, JCYJ20180305180635082, and GJHZ20180928155207206), Open Fund of State Key Laboratory of Applied Optics (grant no. SKLAO-201904), and Guangdong Innovative and Entrepreneurial Research Team Program (grant no. 2017ZT07C071). The authors acknowledge the assistance of SUSTech Core Research Facilities.

■ REFERENCES

(1) Ichimura, K. Photoalignment of Liquid-Crystal Systems. *Chem. Rev.* **2000**, *100*, 1847−1874.
(2) Fuh, A. Y.-G.; Liu, C.-K.; Cheng, K.-T.; Ting, C.-L.; Chen, C.-C.; Chao, P. C.-P.; Hsu, H.-K. Variable Liquid Crystal Pretilt Angles Generated by Photoalignment in Homeotropically Aligned Azo Dye-Doped Liquid Crystals. *Appl. Phys. Lett.* **2009**, *95*, 161104.
(3) Fang, G.; Shi, Y.; Maclennan, J. E.; Clark, N. A.; Farrow, M. J.; Walba, D. M. Photo-Reversible Liquid Crystal Alignment Using Azobenzene-Based Self-Assembled Monolayers: Comparison of the Bare Monolayer and Liquid Crystal Reorientation Dynamics. *Langmuir* **2010**, *26*, 17482−17488.
(4) Yi, Y.; Farrow, M. J.; Korblova, E.; Walba, D. M.; Furtak, T. E. High-Sensitivity Aminoazobenzene Chemisorbed Monolayers for Photoalignment of Liquid Crystals. *Langmuir* **2009**, *25*, 997−1003.
(5) Prompinit, P.; Achalkumar, A. S.; Bramble, J. P.; Bushby, R. J.; Wälti, C.; Evans, S. D. Controlling Liquid Crystal Alignment Using Photocleavable Cyanobiphenyl Self-Assembled Monolayers. *ACS Appl. Mater. Interfaces* **2010**, *2*, 3686−3692.
(6) Janning, J. L. Thin Film Surface Orientation for Liquid Crystals. *Appl. Phys. Lett.* **1972**, *21*, 173−174.
(7) Liu, Y. J.; Loh, W. W.; Leong, E. S. P.; Kustandi, T. S.; Sun, X. W.; Teng, J. H. Nanoimprinted Ultrafine Line and Space Nanogratings for Liquid Crystal Alignment. *Nanotechnology* **2012**, *23*, 465302.
(8) Atkuri, H. M.; Leong, E. S. P.; Hwang, J.; Palermo, G.; Si, G.; Wong, J.-M.; Chien, L.-C.; Ma, J.; Zhou, K.; Liu, Y. J.; De Sio, L. Developing Novel Liquid Crystal Technologies for Display and Photonic Applications. *Displays* **2015**, *36*, 21−29.
(9) Si, G.; Leong, E. S.; Jiang, X.; Lv, J.; Lin, J.; Dai, H.; Liu, Y. J. All-Optical, Polarization-Insensitive Light Tuning Properties in Silver Nanorod Arrays Covered with Photoresponsive Liquid Crystals. *Phys. Chem. Chem. Phys.* **2015**, *17*, 13223−13227.
(10) Hwang, S.-J.; Jeng, S.-C.; Yang, C.-Y.; Kuo, C.-W.; Liao, C.-C. Characteristics of Nanoparticle-Doped Homeotropic Liquid Crystal Devices. *J. Phys. D: Appl. Phys.* **2009**, *42*, No. 025102.
(11) Porte, G. Tilted Alignment of MBBA Induced by Short-Chain Surfactants. *J. Phys.* **1976**, *37*, 1245−1252.
(12) Campanelli, A. R.; Scaramuzza, L. Hexadecyltrimethylammonium Bromide. *Acta Crystallogr., Sect. C: Cryst. Struct. Commun* **1986**, *42*, 1380−1383.
(13) Kang, D.; Rosenblatt, C. Surface-Anisotropy-Induced Linear Electro-optic Effect in a Nematic Liquid Crystal. *Phys. Rev. E* **1996**, *53*, 2976−2979.
(14) Jeng, S.-C.; Hwang, S.-J.; Yang, C.-Y. Tunable Pretilt Angles Based on Nanoparticles-Doped Planar Liquid-Crystal Cells. *Opt. Lett.* **2009**, *34*, 455−457.
(15) Kim, K.-H.; Park, B. W.; Choi, S.-W.; Lee, J.-H.; Kim, H.; Shin, K.-C.; Kim, H. S.; Yoon, T.-H. Vertical Alignment of Liquid Crystals Without Alignment Layers. *Liq. Cryst.* **2013**, *40*, 391−395.
(16) Russell, J. M.; Oh, S.; LaRue, I.; Zhou, O.; Samulski, E. T. Alignment of Nematic Liquid Crystals Using Carbon Nanotube Films. *Thin Solid Films* **2006**, *509*, 53−57.
(17) Kuo, C.-W.; Jeng, S.-C.; Wang, H.-L.; Liao, C.-C. Application of Nanoparticle-Induced Vertical Alignment in Hybrid-Aligned Nematic Liquid Crystal Cell. *Appl. Phys. Lett.* **2007**, *91*, 141103.
(18) Lu, S.-Y.; Chien, L.-C. Carbon Nanotube Doped Liquid Crystal OCB Cells: Physical and Electro-optical Properties. *Opt. Express* **2008**, *16*, 12777−12785.
(19) Qi, H.; Hegmann, T. Multiple Alignment Modes for Nematic Liquid Crystals Doped with Alkylthiol-Capped Gold Nanoparticles. *ACS Appl. Mater. Interfaces* **2009**, *1*, 1731−1738.
(20) Jeng, S.-C.; Kuo, C.-W.; Wang, H.-L.; Liao, C.-C. Nanoparticle-Induced Vertical Alignment in Liquid Crystal Cell. *Appl. Phys. Lett.* **2007**, *91*, No. 061112.
(21) Yoon, W. J.; Lee, K. M.; Evans, D. R.; McConney, M. E.; Kim, D. Y.; Jeong, K.-U. Giant Surfactants for the Construction of Automatic Liquid Crystal Alignment Layers. *J. Mater. Chem. C* **2019**, *7*, 8500−8514.
(22) Shiraishi, Y.; Toshima, N.; Maeda, K.; Yoshikawa, H.; Xu, J.; Kobayashi, S. Frequency Modulation Response of a Liquid-Crystal Electro-optic Device Doped with Nanoparticles. *Appl. Phys. Lett.* **2002**, *81*, 2845−2847.
(23) Lee, W.; Wang, C.-Y.; Shih, Y.-C. Effects of Carbon Nanosolids on the Electro-optical Properties of a Twisted Nematic Liquid-Crystal Host. *Appl. Phys. Lett.* **2004**, *85*, 513−515.
(24) Park, H.-G.; Lee, J.-J.; Dong, K.-Y.; Oh, B.-Y.; Kim, Y.-H.; Jeong, H.-Y.; Ju, B.-K.; Seo, D.-S. Homeotropic Alignment of Liquid Crystals on a Nano-Patterned Polyimide Surface Using Nanoimprint Lithography. *Soft Matter* **2011**, *7*, 5610−5614.
(25) Wang, X.; Wang, H.; Luo, L.; Huang, J.; Gao, J.; Liu, X. Dependence of Pretilt Angle on Orientation and Conformation of Side Chain with Different Chemical Structure in Polyimide Film Surface. *RSC Adv.* **2012**, *2*, 9463−9472.
(26) Kawatsuki, N.; Takatsuka, H.; Kawakami, Y.; Yamamoto, T. Photo-alignment of Low-Molecular Liquid Crystals on Photo-Crosslinkable Polymer Liquid Crystalline Film by Linearly Polarised UV Light. *Polym. Adv. Technol.* **1999**, *10*, 429−433.
(27) Ikeda, T. Photomodulation of Liquid Crystal Orientations for Photonic Applications. *J. Mater. Chem.* **2003**, *13*, 2037−2057.
(28) Sato, M.; Nagano, S.; Seki, T. A Photoresponsive Liquid Crystal Based on (1-cyclohexenyl)phenyldiazene as a Close Analogue of Azobenzene. *Chem. Commun.* **2009**, 3792−3794.
(29) Yaroshchuk, O.; Reznikov, Y. Photoalignment of Liquid Crystals: Basics and Current Trends. *J. Mater. Chem.* **2012**, *22*, 286−300.
(30) Yu, H.; Ikeda, T. Photocontrollable Liquid-Crystalline Actuators. *Adv. Mater.* **2011**, *23*, 2149−2180.
(31) Mizusaki, M.; Nakanishi, Y.; Enomoto, S. Fabrication of Vertically Aligned Liquid Crystal Cell Without Using a Conventional Alignment Layer. *Liq. Cryst.* **2017**, *45*, 270−278.
(32) He, R.; Wen, P.; Kang, S.-W.; Lee, S. H.; Lee, M.-H. Polyimide-Free Homogeneous Photoalignment Induced by Polymerisable Liquid Crystal Containing Cinnamate Moiety. *Liq. Cryst.* **2018**, *45*, 1342−1352.
(33) Mizusaki, M. Fabrication of Vertical Alignment Liquid Crystal Cell Without Forming a Conventional Polyimide-Alignment Layer. *Liq. Cryst.* **2018**, *46*, 1167−1174.

(34) Park, C.; Lee, J.; Kim, C. Functional Supramolecular Assemblies Derived from Dendritic Building Blocks. *Chem. Commun.* **2011**, *47*, 12042−12056.
(35) Kosa, T.; Sukhomlinova, L.; Su, L.; Taheri, B.; White, T. J.; Bunning, T. J. Light-Induced Liquid Crystallinity. *Nature* **2012**, *485*, 347−349.
(36) Tanaka, D.; Ishiguro, H.; Shimizu, Y.; Uchida, K. Thermal and Photoinduced Liquid Crystalline Phase Transitions with a Rod−Disc Alternative Change in the Molecular Shape. *J. Mater. Chem.* **2012**, *22*, 25065−25071.
(37) Wang, G.; Zhang, M.; Zhang, T.; Guan, J.; Yang, H. Photoresponsive Behaviors of Smectic Liquid Crystals Tuned by an Azobenzene Chromophore. *RSC Adv.* **2012**, *2*, 487−493.
(38) Wu, M.-H.; Chu, C.-C.; Cheng, M.-C.; Hsiao, V. K. S. Reversible Phase Transition and Rapid Switching of Azobenzene-Doped Cholesteric Liquid Crystals with a Single Laser. *Mol. Cryst. Liq. Cryst.* **2012**, *557*, 176−189.
(39) Wie, J. J.; Lee, K. M.; Smith, M. L.; Vaia, R. A.; White, T. J. Torsional Mechanical Responses in Azobenzene Functionalized Liquid Crystalline Polymer Networks. *Soft Matter* **2013**, *9*, 9303−9310.
(40) Kundu, S.; Lee, M. H.; Lee, S. H.; Kang, S. W. In situ Homeotropic Alignment of Nematic Liquid Crystals Based on Photoisomerization of Azo-Dye, Physical Adsorption of Aggregates, and Consequent Topographical Modification. *Adv. Mater.* **2013**, *25*, 3365−3370.
(41) Yoon, W.-J.; Choi, Y.-J.; Kim, D.-Y.; Kim, J. S.; Yu, Y.-T.; Lee, H.; Lee, J.-H.; Jeong, K.-U. Photopolymerization of Reactive Amphiphiles: Automatic and Robust Vertical Alignment Layers of Liquid Crystals with a Strong Surface Anchoring Energy. *Macromolecules* **2016**, *49*, 23−29.
(42) Pozhidaev, E.; Chigrinov, V.; Li, X. Photoaligned Ferroelectric Liquid Crystal Passive Matrix Display with Memorized Gray Scale. *Jpn. J. Appl. Phys.* **2006**, *45*, 875−882.
(43) Yaroshchuk, O.; Kyrychenko, V.; Tao, D.; Chigrinov, V.; Kwok, H. S.; Hasebe, H.; Takatsu, H. Stabilization of Liquid Crystal Photoaligning Layers by Reactive Mesogens. *Appl. Phys. Lett.* **2009**, *95*, No. 021902.
(44) Guo, Q.; Srivastava, A. K.; Chigrinov, V. G.; Kwok, H. S. Polymer and Azo-Dye Composite: a Photo-Alignment Layer for Liquid Crystals. *Liq. Cryst.* **2014**, *41*, 1465−1472.
(45) Glushchenko, A.; Kresse, H.; Reshetnyak, V.; Reznikov, Y.; Yaroshchuk, O. Memory Effect in Filled Nematic Liquid Crystals. *Liq. Cryst.* **2010**, *23*, 241−246.
(46) Kumar, V.; Nasrollahi, A.; Baliyan, V. K.; Park, H.-S.; Lee, M.-H.; Kang, S.-W. Dual Wavelength in situ Photoalignment for Stable Planar Alignment of Nematic Liquid Crystals. *Opt. Mater. Express* **2018**, *8*, 2366−2377.
(47) Nasrollahi, A.; Kumar, V.; Lee, M. H.; Kang, S. W.; Park, H. S.; Lim, H.; Chan Oh, K.; Lyu, J. J. Polyimide-Free Planar Alignment of Nematic Liquid Crystals: Sequential Interfacial Modifications through Dual-Wavelength in Situ Photoalignment. *ACS Appl. Mater. Interfaces* **2019**, *11*, 15141−15151.
(48) Liu, Y. J.; Zheng, Y. B.; Shi, J.; Huang, H.; Walker, T. R.; Huang, T. J. Optically Switchable Gratings Based on Azo-Dye-Doped Polymer-dispersed liquid crystals. *Opt. Lett.* **2009**, *34*, 2351−2353.
(49) Liu, Y. J.; Zheng, Y. B.; Liou, J.; Chiang, I.-K.; Khoo, I. C.; Huang, T. J. All-Optical Modulation of Localized Surface Plasmon Coupling in a Hybrid System Composed of Photo-Switchable Gratings and Au Nanodisk Arrays. *J. Phys. Chem. C* **2011**, *115*, 7717−7722.
(50) Liu, Y. J.; Dai, H. T.; Leong, E. S. P.; Teng, J. H.; Sun, X. W. Azo-Dye-Doped Absorbing Photonic Crystals with Purely Imaginary Refractive Index Contrast and All-Optically Switchable Diffraction Properties. *Opt. Mater. Express* **2012**, *2*, 55−61.
(51) Kim, S. G.; Kim, S. M.; Kim, Y. S.; Lee, H. K.; Lee, S. H.; Lee, G. D.; Lyu, J. J.; Kim, K. H. Stabilization of the Liquid Crystal Director in the Patterned Vertical Alignment Mode Though Formation of Pretilt Angle by Reactive Mesogen. *Appl. Phys. Lett.* **2007**, *90*, 261910.
(52) Kim, D.-Y.; Lee, S.-A.; Kim, S.; Nah, C.; Lee, S. H.; Jeong, K.-U. Asymmetric Fullerene Nanosurfactant: Interface Engineering for Automatic Molecular Alignments. *Small* **2017**, *14*, 1702439.
(53) Yoon, W.-J.; Choi, Y.-J.; Kang, D.-G.; Kim, D.-Y.; Park, M.; Lee, J.-H.; Jeong, K.-U. Construction of Polymer-Stabilized Automatic Multidomain Vertical Molecular Alignment Layers with Pretilt Angles by Photopolymerizing Dendritic Monomers under Electric Fields. *ACS Omega* **2017**, *2*, 5942−5948.
(54) Moon, Y.-K.; Lee, Y.-J.; Jo, S. I.; Kim, Y.; Heo, J. U.; Baek, J.-H.; Kang, S.-G.; Yu, C.-J.; Kim, J.-H. Effects of Surface Modification with Reactive Mesogen on the Anchoring Strength of Liquid Crystals. *J. Appl. Phys.* **2013**, *113*, 234504.
(55) Lim, Y. J.; Woo, C. W.; Oh, S. H.; Mukherjee, A.; Lee, S. H.; Baek, J. H.; Kim, K. J.; Yang, M. S. Enhanced Contrast Ratio of Homogeneously Aligned Liquid Crystal Displays by Controlling the Surface-Anchoring Strength. *J. Phys. D: Appl. Phys.* **2011**, *44*, 325403.
(56) Tie, W.; Jeong, I. H.; Jang, I. W.; Han, J. S.; Liu, Y.; Li, X. D.; Lee, M. H.; Jeong, K.-U.; Lee, S. H. Reducing Driving Voltage and Securing Electro-optic Reliability of In-plane Switching Liquid Crystal Display by Applying Polysulfone Photoalignment Layer with Photo-reactive Mesogens. *Liq. Cryst.* **2014**, *41*, 1057−1064.
(57) Son, I.; Lee, B.; Kim, C.; Kim, J. H.; Yoo, J. Y.; Lee, J. H. In situ Self-Assembled Homeotropic Alignment Layer for Fast-Switching Liquid Crystal Devices. *Liq. Cryst.* **2016**, *43*, 517−523.
(58) Son, I.; Kim, J. H.; Kim, C.; Lee, B.; Yoo, J. Y.; Cho, C. H.; Lee, J. H. Self-assembled Vertical Alignment Layer of Bifunctional Amphiphiles for Fast Electro-optical Switching of Nematic Liquid Crystals. *Mol. Cryst. Liq. Cryst.* **2017**, *659*, 52−58.
(59) Yokoyama, H.; van Sprang, H. A. A Novel Method for Determining the Anchoring Energy Function at a Nematic Liquid Crystal-Wall Interface from Director Distributions at High Fields. *J. Appl. Phys.* **1985**, *57*, 4520−4526.
(60) Nie, X.; Lin, Y.-H.; Wu, T. X.; Wang, H.; Ge, Z.; Wu, S. T. Polar Anchoring Energy Measurement of Vertically Aligned Liquid-Crystal Cells. *J. Appl. Phys.* **2005**, *98*, No. 013516.

https://dx.doi.org/10.1021/acsaelm.0c00295
ACS Appl. Electron. Mater. 2020, 2, 2017−2025